Article **ECORFAN Journal**

Engineering June 2015 Vol.2 No.2 80-91

Calculation of Dynamic Properties of Hybrid Supports of injected lubricant. Analytical Development

RAMIREZ, Ignacio*†, JARAMILLO, Jesús y RECIO-CAMPOS, Celeste

Instituto Tecnológico de Pachuca. División de Estudios de Posgrado e Investigación. Carretera México-Pachuca Km 87.5, Col. Venta Prieta, Pachuca de Soto, Hidalgo. MEXICO. Teléfono (771) 711 3140, extensión 139

Received January 8, 2014; Accepted June 12, 2015

Abstract

In this work we obtain analytical expressions for the calculation of the stiffness and damping of a short journal bearing, which is being submitted to an external pressurization force. These expressions are obtained from Reynolds equation, which is modified to model the effect of pressurization. Such modification lies in the introduction of a generalized function of the space impulse type (Dirac Delta). It is important to mention that such modeling is first in its kind to solve rotodynamic problems. Additionally there are graphics showing the performance of the stiffness and damping coefficients as a function of the eccentricity and/or externalpressurization. It is important to notice that this is the first work that reports analytical results of such coefficients being modified by the effect of pressurization; currently there are only numerical solutions for its calculation. Also, the dynamic behavior of a rotatory system is highly influenced by the values that may be taken by the coefficients of stiffness and damping; therefore, if the dependence to pressurization is known, it is possible to determine the pressure values that may be applied until instability is reached

Bearing, Pressurization, Coefficients Rotodynamic, Stiffness, Damping.

Citation: RAMIREZ, Ignacio, JARAMILLO, Jesús y RECIO-CAMPOS, Celeste. Calculation of Dynamic Properties of Hybrid Supports of injected lubricant. Analytical Development. ECORFAN Journal-Bolivia 2015, 2-2: 80-91

* Correspondence to Author (email: tijonov@hotmail.com)
† Researcher contributing first author.

Introduction

The equations of motion of rotor-bearings, system contain coefficients corresponding to the film of the lubricant of the bearings, these parameters change with the rotational speed and consequently also change with the addition of external pressure. That's why the dynamic behavior is always heavily influenced by the values they can take these coefficients. It is in the literature as the operation speed increases, one of the stiffness coefficients can take negative values depending on its magnitude and the system could instability [1].

To study the behavior of the fluid in the hydrodynamic bearings Reynolds equation is used, which is a simplification of the Navier-Stokes equations for Newtonian fluids type. Reynolds equation relates the fluid pressure in the bearing with axial and circumferential coordinates, so that using this equation; it is possible to obtain the pressure field. Unable to resolve analytically Reynolds equation, but can be obtained depending on the ratio approaches. (L / D); which indicates whether the bearing is short or long. Therefore, if the Reynolds equation is modified by a generalized function of spatial impulse (Dirac) that models the external lubricant injection, be possible to find an expression that determines the pressure field in the fluid film as a function of pressurizing external and in turn determine the stiffness and damping forces and corresponding coefficients, also called coefficients rotordynamic.

Classic definition of the aerodynamic coefficients

The model describing the function of pressure in hydrodynamic bearings is the Reynolds equation, such an equation can be written generally as [2]:

$$\frac{\partial}{\partial\theta}\left[h^3\frac{\partial p}{\partial\theta}\right]+R^2\frac{\partial}{\partial z}\left[h^3\frac{\partial p}{\partial z}\right]=12\frac{\mu R^2}{C_r^2}\left[C_1\varepsilon Cos\theta+C_2\varepsilon(\varphi-\frac{\omega}{2})Sen\theta\right] \quad (1)$$

$$-\frac{L}{2}\le z\le\frac{L}{2},\quad 0\le\theta\le 2\pi,\quad h(\theta)=1+\varepsilon Cos\theta \quad (2)$$

$$p(\frac{L}{2})=0;\ p(-\frac{L}{2})=0;\ p(\theta+2\pi)=p(\theta) \quad (3)$$

Where $p:$ is the pressure in the lubricant film, $h:$ is the dimensionless film thickness of the fluid, $R:$ is the radius of the bearing represents the radial course, $C_r:$ is the bearing length, $L:$ is the equilibrium angle (attitud), $\varphi:$ is the dimensionless eccentricity of the bearing $\varepsilon:$ is the lubricant viscosity fluid, $\mu:$ is the angular coordinate in any point of the bearing and the axial coordinate of the bearing.

To work in general, it is possible dimensionless Reynolds equation using the following substitutions:

$$z=\frac{L}{2}\bar{z}\qquad p=\mu N\left(\frac{R}{Cr}\right)^2\bar{p}$$

$$N=\frac{\omega}{2\pi}\qquad \hat{p}=\frac{\bar{p}}{(1-2\dot{\phi}/\omega)} \quad (4)$$

Then leaving:

$$\frac{\partial}{\partial\theta}\left[h^3\frac{\partial\hat{p}}{\partial\theta}\right]+\left(\frac{D}{L}\right)^2\frac{\partial}{\partial\bar{z}}\left[h^3\frac{\partial\hat{p}}{\partial\bar{z}}\right]=24\pi\frac{\dot{\varepsilon}/\omega}{(1-2\dot{\phi}/\omega)}Cos\theta-12\pi\varepsilon Sen\theta \quad (5)$$

However, in this work the main interest is in short bearings, which comply with the condition: $L/D<1/2$.

For both the first member of (5), the first term is small compared to the second and so dimensionless Reynolds equation for short bearings remain as:

ISSN-On line: 2410-4191

$$\left(\frac{D}{L}\right)^2 \frac{\partial}{\partial \bar{z}}\left[h^3 \frac{\partial \hat{p}}{\partial \bar{z}}\right] = 24\pi \frac{\dot{\varepsilon}/\omega}{(1-2\dot{\varphi}/\omega)} Cos\theta - 12\pi\varepsilon Sen\theta \quad (6)$$

Once resolved (6), the dimensional components of force in the radial and transverse directions are:

$$\bar{F}_R = \frac{F_R}{\mu NLD(R/C_r)^2} = (1-2\dot{\varphi}/\omega) f_R \quad (7)$$

$$\bar{F}_T = \frac{F_T}{\mu NLD(R/C_r)^2} = (1-2\dot{\varphi}/\omega) f_T \quad (8)$$

$$f_R = \frac{1}{4}\int_{-1}^{1}\int_{0}^{\pi} \hat{p}(\theta,\bar{z}) Cos\theta \, d\theta \, d\bar{z} \quad (9)$$

$$f_T = \frac{1}{4}\int_{-1}^{1}\int_{0}^{\pi} \hat{p}(\theta,\bar{z}) Sen\theta \, d\theta \, d\bar{z} \quad (10)$$

The following expression relates the resultant force f_R and f_T to obtain a very important dimensionless number in rotodynamic:

$$S = \frac{1}{\sqrt{f_R^2 + f_T^2}} = \frac{\mu NLD}{W}\left(\frac{R}{C_r}\right)^2 = \frac{F_{\dim}}{W} \quad (11)$$

This number is called Sommerfeld number and the geometrical characteristics relating lubricant viscosity and the bearings of the hydrodynamic forces and weight.

The change of forces fR and fT around the equilibrium position provides stiffness and damping coefficients, which are defined by [3]:

$$\bar{K} = \begin{pmatrix} \frac{\partial f_R}{\partial \varepsilon} & \frac{\partial f_R}{\varepsilon \partial \varphi} - \frac{f_T}{\varepsilon} \\ \frac{\partial f_T}{\partial \varepsilon} & \frac{\partial f_T}{\varepsilon \partial \varphi} + \frac{f_R}{\varepsilon} \end{pmatrix} = \begin{pmatrix} K_{RR} & K_{RT} \\ K_{TR} & K_{TT} \end{pmatrix}$$

$$\bar{C} = \begin{pmatrix} \frac{\partial f_R}{\partial(\dot{\varepsilon}/\omega)} & -\frac{2 f_R}{\varepsilon} \\ \frac{\partial f_T}{\partial(\dot{\varepsilon}/\omega)} & -\frac{2 f_T}{\varepsilon} \end{pmatrix} = \begin{pmatrix} C_{RR} & C_{RT} \\ C_{TR} & C_{TT} \end{pmatrix} \quad (12)$$

$$(13)$$

Where $[\bar{K}]$ It is the matrix of the coefficients of stiffness and $[\bar{C}]$ is the matrix of coefficients buffer. These coefficients are related to its dimensional part by:

$$\bar{K}_{ij} = \left[\frac{C_r}{\mu NLD\left(R/C_r\right)^2}\right] K_{ij}$$

$$\bar{C}_{ij} = \left[\frac{\omega C_r}{\mu NLD\left(R/C_r\right)^2}\right] C_{ij} \quad (14)$$

Note that the thermodynamic coefficients given by (12) and (13) are referred to the system of radial and transverse coordinates, if you wanted to obtain these coefficients with respect to another coordinate system is only necessary to multiply by the corresponding rotation matrix.

Generally the coefficients of stiffness and damping are presented in the literature as:

$$\tilde{K}_{ij} = \left(\frac{C_r}{W}\right) K_{ij}$$

$$\tilde{C}_{ij} = \left(\frac{\omega C_r}{W}\right) C_{ij} \quad (15)$$

The relationship between (14) and (15) is through the Sommerfeld number given by (11) where:

$$\tilde{K}_{ij} = S\bar{K}_{ij}$$

$$\tilde{C}_{ij} = S\bar{C}_{ij} \quad (16)$$

ISSN-On line: 2410-4191

Solution for short bearings

External no pressurization

The mathematical model of a short bearing without external pressurization is given by (6) where the solution comes by:

$$\hat{p}=\left(\frac{L}{D}\right)^2\frac{6\pi\left(1-\bar{z}^2\right)}{\left(1+\varepsilon Cos\theta\right)^3}\left[\varepsilon Sen\theta-2\frac{\dot{\varepsilon}/\omega}{\left(1-2\dot{\varphi}/\omega\right)}Cos\theta\right] \tag{17}$$

Substituting (17) into (9) and (10), it is known that the dimensionless forces are:

$$f_R=\left(\frac{L}{D}\right)^2\left\{\frac{-4\pi\varepsilon^2}{\left(1-\varepsilon^2\right)^2}-\frac{2\pi^2\left(1+2\varepsilon^2\right)}{\left(1-\varepsilon^2\right)^{5/2}}\cdot\frac{\dot{\varepsilon}/\omega}{\left(1-2\dot{\varphi}/\omega\right)}\right\} \tag{18}$$

$$f_T=\left(\frac{L}{D}\right)^2\left\{\frac{\pi^2\varepsilon}{\left(1-\varepsilon^2\right)^{3/2}}+\frac{8\pi\varepsilon}{\left(1-\varepsilon^2\right)^2}\cdot\frac{\dot{\varepsilon}/\omega}{\left(1-2\dot{\varphi}/\omega\right)}\right\} \tag{19}$$

Thus, it is possible to find the coefficients of stiffness and damping in the radial and transverse directions of a short bearing no pressurization, only substituting (18) and (19) (12) and (13). After multiplying by the corresponding rotation matrix and using (16), the coefficients are obtained in the rectangular coordinate system. See Table 1.

$\tilde{k}_{xx}=\frac{4\left[\pi^2+\left(32+\pi^2\right)\varepsilon^2+2\left(16-\pi^2\right)\varepsilon^4\right]}{\left(1-\varepsilon^2\right)\left[\pi^2+\left(16-\pi^2\right)\varepsilon^2\right]^{3/2}}$	$\tilde{c}_{xx}=\frac{2\pi\left[\pi^2+2\left(24-\pi^2\right)\varepsilon^2+\pi^2\varepsilon^4\right]}{\varepsilon\sqrt{1-\varepsilon^2}\left[\pi^2+\left(16-\pi^2\right)\varepsilon^2\right]^{3/2}}$
$\tilde{k}_{xy}=\frac{\pi\left[\pi^2+\left(32+\pi^2\right)\varepsilon^2+2\left(16-\pi^2\right)\varepsilon^4\right]}{\varepsilon\sqrt{1-\varepsilon^2}\left[\pi^2+\left(16-\pi^2\right)\varepsilon^2\right]^{3/2}}$	$\tilde{c}_{xy}=\frac{8\left[\pi^2+2\left(\pi^2-8\right)\varepsilon^2\right]}{\left[\pi^2+\left(16-\pi^2\right)\varepsilon^2\right]^{3/2}}$
$\tilde{k}_{yx}=\frac{\pi\left[-\pi^2+2\pi^2\varepsilon^2+\left(16-\pi^2\right)\varepsilon^4\right]}{\varepsilon\sqrt{1-\varepsilon^2}\left[\pi^2+\left(16-\pi^2\right)\varepsilon^2\right]^{3/2}}$	$\tilde{c}_{yx}=\frac{8\left[\pi^2+2\left(\pi^2-8\right)\varepsilon^2\right]}{\left[\pi^2+\left(16-\pi^2\right)\varepsilon^2\right]^{3/2}}$
$\tilde{k}_{yy}=\frac{4\left[2\pi^2+\left(16-\pi^2\right)\varepsilon^2\right]}{\left[\pi^2+\left(16-\pi^2\right)\varepsilon^2\right]^{3/2}}$	$\tilde{c}_{yy}=\frac{2\pi\left(1-\varepsilon^2\right)^{1/2}\left[\pi^2+2\left(\pi^2-8\right)\varepsilon^2\right]}{\varepsilon\left[\pi^2+\left(16-\pi^2\right)\varepsilon^2\right]^{3/2}}$

Table 1 Aerodynamic coefficients of stiffness and damping for short bearings in the XY system

With external pressurization

Now you need to enter the external pressurization effect and is important to specify the axial and circumferential injection point. This article is modeled using external pressurization function space Delta Dirac impulse $\delta(x)$ (also called generalized function or distribution), which has special properties that help in solving the model.

Suppose the pressurization will be given a mathematical point that such behavior is modeled perfectly by the pulse function. This can be generalized for injections "n" arbitrary points of the bearing. Therefore, it is possible to consider incorporating the Dirac impulse function as a way to represent the lubricant injection is performed at an arbitrary position [4].

Then the bearing undergoing pressurization, performed in an injection port which axial and circumferential location is arbitrary occurs. See Figure 1.

ISSN-On line: 2410-4191

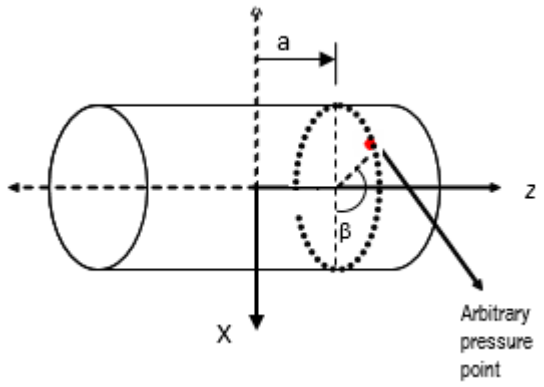

Graphic 1 Location pressurization point in the bearing. Note that the values of the axial and circumferential coordinates to specify the particular point injection lubricant defined.

This case corresponds to pressurizing with timely door on the point with the dimensionless axial coordinate $\bar{z} = a$ and the circumferential coordinate "β",it is noteworthy that the position of the injection port can be as arbitrary as you like for any securities of "a" and "β" it is noteworthy That the position of the injection port can be as arbitrary as you like for any securities of

$$(\Delta\bar{p})_{prt} = \bar{q}_{prt}\delta(\bar{z}-a)\delta\left[\theta-(\pi+\beta-\varphi_{pres})\right] \qquad (20)$$
$$\bar{q}_{prt} = \frac{\Delta F_{pres}}{DL\mu N\left(R/Cr\right)^2} = \frac{\Delta F_{pres}}{F_{\dim}}$$

Note that although the Dirac delta function is defined as infinite impulse at the point of the axial and angular coordinates, the pressurizing force is not equal to infinity since as the injection port is considered a mathematical point, the product of pressure ($\bar{q}_{prt} \to \infty$)the gate area ($\bar{A}_{prt} \to 0$) It will be a constant value.

Equally worth mentioning that the Dirac function in this model does not indicate that the pressure is applied and disappears at a certain time, is it is not a temporary role but is a spatial function for a given value axial and angular coordinate, pressure is applied in pulse form.

It is proposed as the model of pressurization in the spot port, the dimensionless equation:

$$\frac{\partial}{\partial\bar{z}}\left[h^3\frac{\partial\hat{p}}{\partial\bar{z}}\right] = \left(\frac{L}{D}\right)^2\bar{q}_{prt}\delta(\bar{z}-a)\delta\left[\theta-(\pi+\beta-\varphi_{pres})\right]\cdot\frac{1}{\left(1-2\dot{\varphi}/\omega\right)}$$
$$\hat{p}(\bar{z}=\pm1)=0, \quad \hat{p}(\theta+2\pi)=\hat{p}(\theta)$$
$$-1\le\bar{z}\le1, \quad 0\le\theta\le2\pi \qquad (21)$$

Solving to (21) and using the properties of the Dirac delta function is obtained:

$$\hat{p}_{PRES} = \left(\frac{L}{D}\right)^2\bar{q}_{prt}\frac{\delta\left[\theta-(\pi+\beta-\varphi_{pres})\right]}{2\left(1+\varepsilon_{pres}Cos\theta\right)^3}\left[1-a\bar{z}-|\bar{z}-a|\right]\cdot\frac{1}{\left(1-2\dot{\varphi}/\omega\right)} \qquad (22)$$

After replacing (22) in (9) and (10) yields:

$$f_R = -\left(\frac{L}{D}\right)^2\bar{q}_{prt}\frac{\left(1-a^2\right)}{8}\frac{Cos(\beta-\varphi)}{\left[1-\varepsilon Cos(\beta-\varphi)\right]^3}\cdot\frac{1}{\left(1-2\dot{\varphi}/\omega\right)} \qquad (23)$$

$$f_T = -\left(\frac{L}{D}\right)^2\bar{q}_{prt}\frac{\left(1-a^2\right)}{8}\frac{Sen(\beta-\varphi)}{\left[1-\varepsilon Cos(\beta-\varphi)\right]^3}\cdot\frac{1}{\left(1-2\dot{\varphi}/\omega\right)} \qquad (24)$$

Substituting (23) and (24) (12) and (13) and after multiplication by the corresponding rotation matrix, the coefficients rotordynamic due to pressurization are obtained. See Table 2.

ISSN-On line: 2410-4191

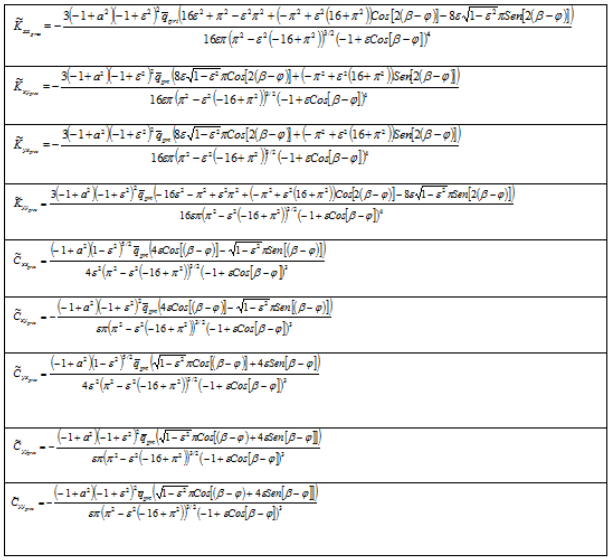

Table 2 Aerodynamic Coefficients stiffness and damping of a short bearing due to external pressurization arbitrary circumferential and axial positions.

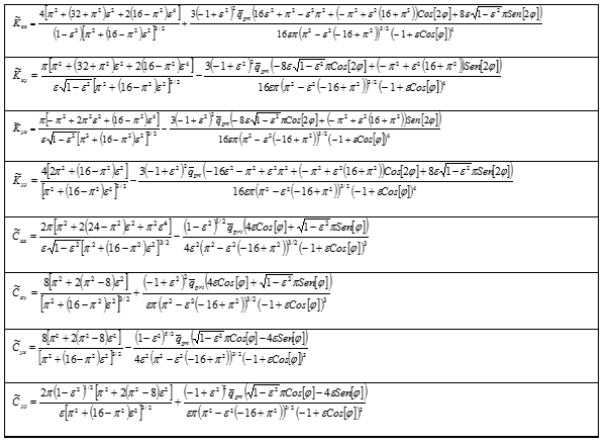

Table 3 Aerodynamic Coefficients complete table of stiffness and damping of pressurized bearing on their part

Table 4 Aerodynamic Coefficients complete table of stiffness and damping of pressurized bearing its top center

Classic case

In the following figures, the conduct of rotordynamic coefficients as a function of the eccentricity of equilibrium for different values of external pressurization force is shown.

Important Note: The dotted lines indicate negative values

1.- $f_{prt} = 0$

When the pressurizing force is zero, is obtained the classic case of the coefficients reported in the literature [2]. In Figures 2 and 3 the rotordynamic coefficients for this case (direct and coupled) appear. Mentioned coefficients were obtained from the formulas given in Table 1, for a short bearing unpressurized externally.

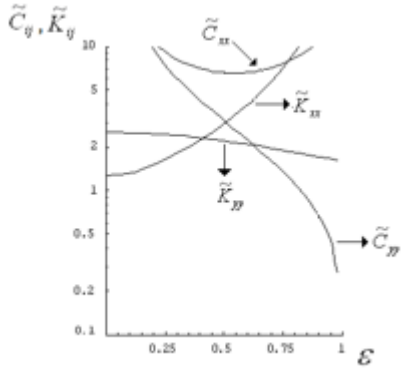

Graphic 2 Direct Aerodynamic coefficients of stiffness and damping for a short bearing unpressurized. $f_{prt} = 0$.

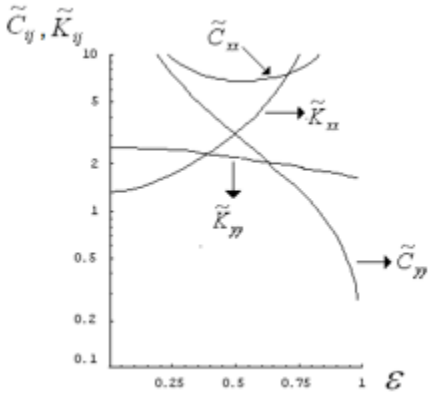

Graphic 3 Coupled Aerodynamic coefficients of stiffness and damping for a short bearing unpressurized. $f_{prt} = 0$.

Pressurized case (Y).

Below the graphs the coefficients of stiffness and damping for different values presented pressurizing force, the above is obtained from the formulas found in Tables 3 and 4.

Lower injection

2.- $f_{prt} = 10$

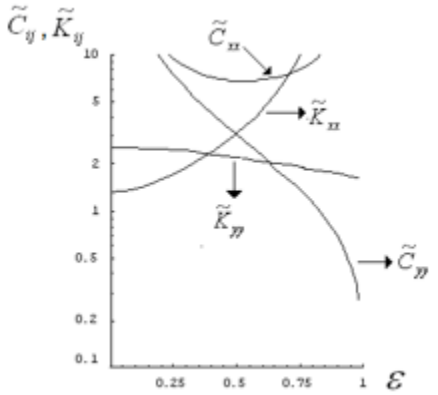

Graphic 4 Direct Aerodynamic coefficients of stiffness and damping for a short bearing pressurized at the bottom. $f_{prt} = 10$.

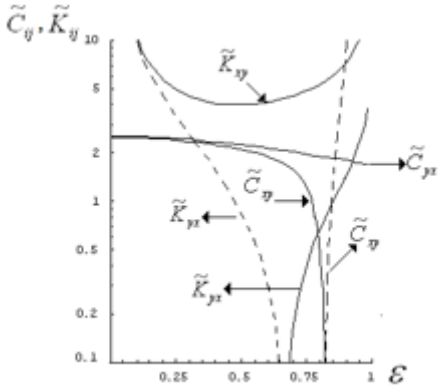

Graphic 5 Aerodynamic Coefficients of Coupled stiffness and damping for a short bearing pressurized at the bottom. $f_{prt} = 10$.

Importantly, Figures 4 and 5, the pressurization causes significant changes only in the coefficients for the vertical directions $\tilde{K}_{xx}, \tilde{C}_{xx}$ and the values of the damping in the directions $\tilde{C}_{xy}$, where not only a separation appears with the coefficient $\tilde{C}_{yx}$ (as it was in Figure 3) but also show negative values for certain ranges of eccentricity, so that they can affect the stability of the system.

In figures 6 through 9 behavior occurs when coefficients rotor dynamic further increases the pressurizing force at the bottom of the bearing.

ISSN-On line: 2410-4191

Note that the graph of damping coefficient $\tilde{C}_{xy}$ (with corresponding negative signs) is going farther and farther to the left for different values of pressurization (Figs. 7 and 9).

3.- $f_{prt} = 100$

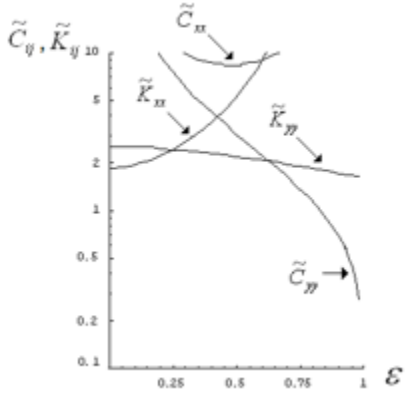

Graphic 6 Direct Aerodynamic coefficients of stiffness and damping for a short bearing pressurized at the bottom. $f_{prt} = 100$.

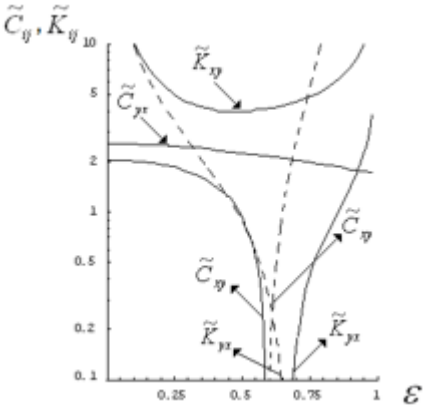

Graphic 7 Aerodynamic Coefficients of Coupled stiffness and damping for a short bearing pressurized at the bottom. $f_{prt} = 100$.

4.- $f_{prt} = 500$

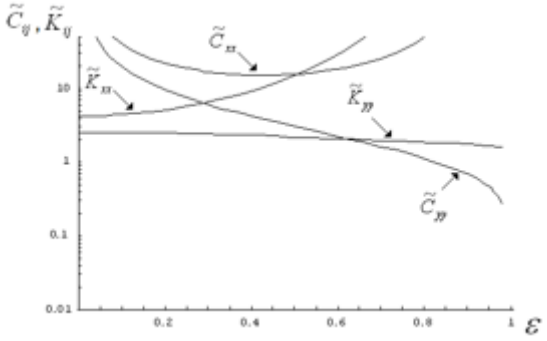

Graphic 8 Aerodynamic coefficients of stiffness and damping for a short bearing pressurized at the bottom. $f_{prt} = 500$.

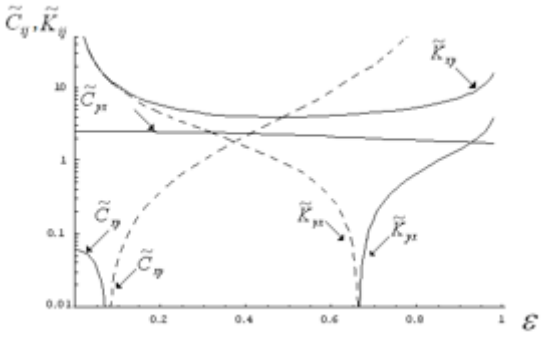

Graphic 9 Coupled Aerodynamic coefficients of stiffness and damping for a short bearing pressurized at the bottom. $f_{prt} = 500$.

Comparison of aerodynamic coefficients (Lower injection)

The following figures show the comparison of rotor dynamic stiffness and damping coefficients (direct in the direction xx) and the buffer (coupled in the x direction) for different values of pressurizing force. Remember that these coefficients are modified to look more drastically when are pressurized externally to the bearing.

Figures 10, 11, 12 and 13 show that the values of stiffness and damping direct in the vertical direction of the lubricant film increases with increasing the strength of external pressurization.

ISSN-On line: 2410-4191

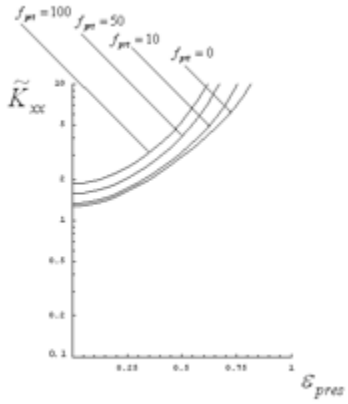

Graphic 10 Comparison of direct aerodynamic coefficients (in the vertical direction) of a short bearing rigidity for different pressurization values bottom.

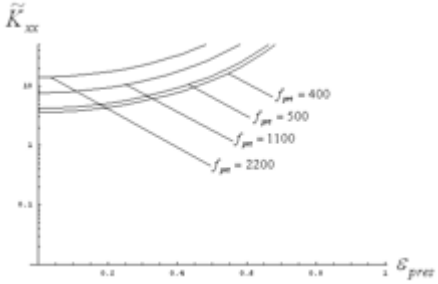

Graphic 11 Direct comparison of aerodynamic coefficients (in the vertical direction) of a short bearing rigidity for different pressurization values bottom.

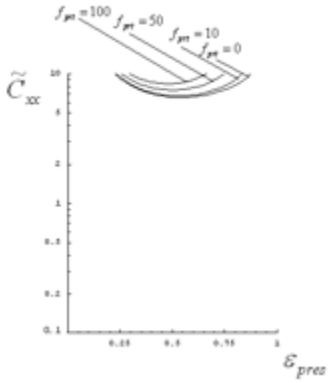

Graphic 12 Direct comparison of aerodynamic coefficients (in the vertical direction) damping of a short bearing for different pressurization values bottom.

Figures 14 and 15 show that as the strength of external pressurization, the damping coefficient in the x direction begins to change sign for certain values of eccentricity and therefore tend to be traveled curves to the left, until it stops values over pressurizing the damping coefficient becomes negative for all possible values of eccentricity, doing this may affect significantly to system stability manner.

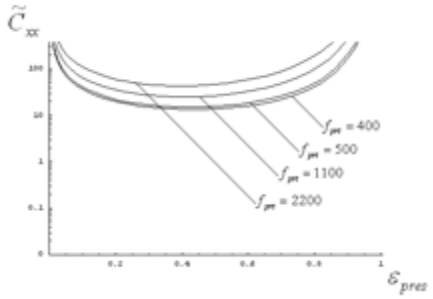

Graphic 13 Comparison of direct rotor dynamic coefficients (in the vertical direction) damping of a short bearing for different pressurization values bottom.

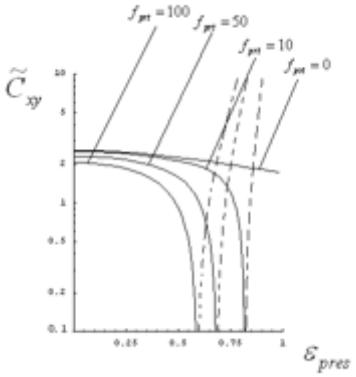

Graphic 14 Comparison of coupled rotor dynamic coefficients (in the x direction) damping of a short bearing for different pressurization values bottom.

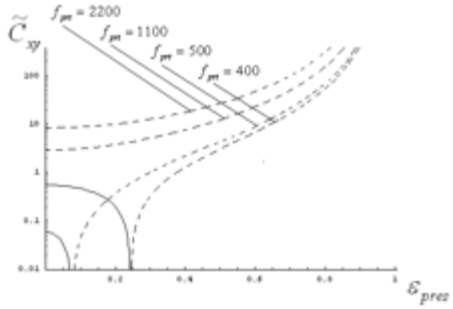

Graphic 15 Comparison of coupled rotor dynamic coefficients (in the x direction) damping of a short bearing for different pressurization values bottom.

ISSN-On line: 2410-4191

Pressurized case (ii)

Superior injection

The following graphic shows this variation for different values of pressurizing force, on top of the bearing.

1.- $f_{prt} = 10$

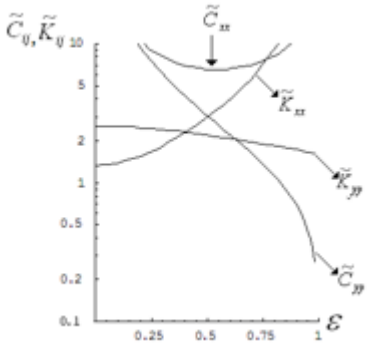

Graphic 16 Direct Rotor dynamic coefficients of stiffness and damping for a short pressurized bearing at the top. $f_{prt} = 10$

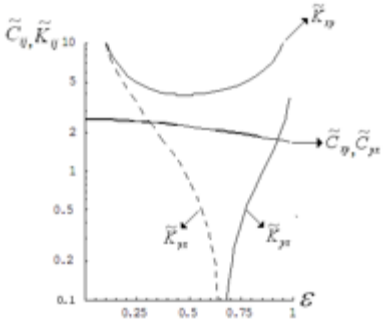

Graphic 17 Rotor dynamic Coefficients of Coupled stiffness and damping for a short pressurized bearing at the top. $f_{prt} = 10$.

As in the previous case (lower injection), the rotor dynamic coefficients are considerably affected are primarily direct in the vertical direction and the buffer $\tilde{C}_{xy}$; which unlike the previous case, it is not negative for any value of eccentricity.

2.- $f_{prt} = 100$

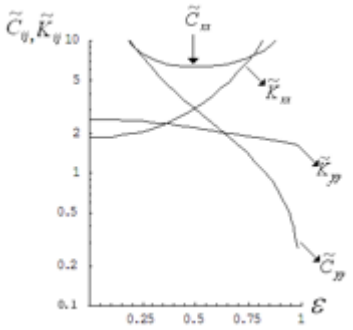

Graphic 18 Direct rotor dynamic coefficients of stiffness and damping for a short pressurized bearing on its top. $f_{prt} = 100$.

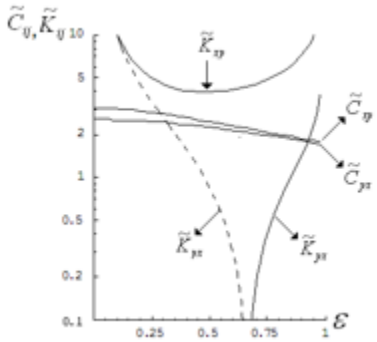

Graphic 19 Rotor dynamic Coefficients of Coupled stiffness and damping for a short pressurized bearing at the top. $f_{prt} = 100$.

Comparison of Rotor dynamic coefficients (Superior Injection)

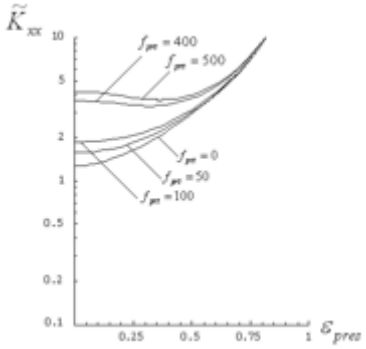

Graphic 20 Comparison of direct rotor dynamic coefficients (in the vertical direction) of a short bearing rigidity for different values of pressurization at the top.

ISSN-On line: 2410-4191

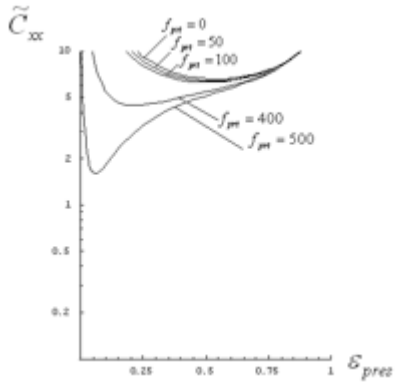

Graphic 21 Comparison of direct rotor dynamic coefficients (in the vertical direction) damping of a short bearing for different values of pressurization at the top.

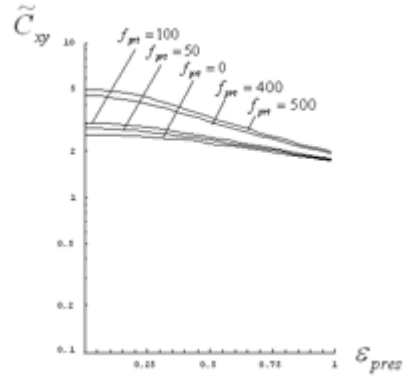

Graphic 22 Comparison of coupled rotor dynamic coefficients (in the x direction) damping of a short bearing for different values of pressurization at the top.

Conclusions

The results found in this work are of fundamental importance, since it was obtained for the first time in international and analytically literature, rotor dynamic coefficients of stiffness and damping as a function of the strength of external pressurization (are summarized in Tables 2 , 3 and 4).

Currently only numeric values of these coefficients are making it less manageable the results; This was possible by using the Dirac external effect pressurization as in equation Reynolds lubrication spatial function.

Graphics behaviors rotor dynamic pressurized coefficients as a function of the eccentricity of balance and pressurizing force in cases where it is pressurized at the bottom and top of the bearing found.

When is pressurized at the bottom, we find that the coefficients of stiffness and direct buffer (in the vertical direction) increase in value as the external pressurizing force is growing, just as the damping coefficient in the x direction is affected in their values when pressurization grows, including changes sign for certain values of eccentricity; This result is of fundamental importance for the stability of the system is determined by the values rotor dynamic having such coefficients, being more conducive to instability as these coefficients take negative values.

Moreover when pressurized at the top of the bearing, the values of the stiffness (in the vertical direction) increase in value as it grows pressurization, but now the damping in the vertical direction decreases when the pressing force grows . Similarly, the damping coefficient in the x direction increases to values greater than the pressing force.

Referencies

A. Antonio García, V. Nosov, J. Gómez Mancilla (2002) "Comparación de coeficientes Rotodinámicos de chumaceras hidrodinámicas usando la teoría de chumaceras a largas, cortas y Warner" 3° Congreso Internacional de Ingeniería Electromecánica y de Sistemas IPN.

Childs, D., (1993)"Turbomachinery Rotor dynamics: Phenomena, Modeling,& Analysis," John Wiley&Sons, NY.

Szeri. (1998) Fluid Film Lubricatión. Theory and Design Cambridge University Press.

ISSN-On line: 2410-4191

V. Nosov, I. Ramírez Vargas, J. Gómez Mancilla (2005). "New model and Stationary Position for a Short Journal Bearings with Point Injection Ports". To be evaluate in the Journal of Turbomachinery.

I. Ramirez Vargas, V.R.Nosov, J. Gómez Mancilla (2004). "Campos de presión de lubricante en chumacera híbrida presurizada con anillo y/o línea unidimensional de presurización", 8° Congreso Nacional de Ingeniería Electromecánica y de Sistemas IPN

Bently D, Petchnev (2000) "Dynamic stiffness and advantages of externally pres-surized fluid film bearings", Orbit, First Quarter.

Khonsari, M.M., Booser, E.R. (2001) "Applied Tribology: Bearing Design and Lubrication," John Wiley & Sons.

Arfken (2000), Mathematical Methods for Physic, AcademicPress 5ta Ed.

ISSN-On line: 2410-4191